the plant journal

SEB Society for Experimental Biology

The Plant Journal (2015) **81,** 329–346 doi: 10.1111/tpj.12730

Absence of SUN1 and SUN2 proteins in *Arabidopsis thaliana* leads to a delay in meiotic progression and defects in synapsis and recombination

Javier Varas[1,†], Katja Graumann[2,†], Kim Osman[3,†], Mónica Pradillo[1], David E. Evans[2], Juan L. Santos[1] and Susan J. Armstrong[3,*]

[1]*Departamento de Genética, Facultad de Biología, Universidad Complutense de Madrid, Madrid 28040, Spain,*
[2]*Department of Biological and Medical Sciences, Faculty of Health and Life Sciences, Oxford Brookes University, Headington Campus, Oxford OX3 OBP, UK, and*
[3]*School of Biosciences, University of Birmingham, Birmingham B15 2TT, UK*

Received 15 August 2014; revised 25 October 2014; accepted 17 November 2014; published online 21 November 2014.
*For correspondence (e-mail s.j.armstrong@bham.ac.uk).
†These authors contributed equally to this work.

SUMMARY

The movement of chromosomes during meiosis involves location of their telomeres at the inner surface of the nuclear envelope. Sad1/UNC-84 (SUN) domain proteins are inner nuclear envelope proteins that are part of complexes linking cytoskeletal elements with the nucleoskeleton, connecting telomeres to the force-generating mechanism in the cytoplasm. These proteins play a conserved role in chromosome dynamics in eukaryotes. Homologues of SUN domain proteins have been identified in several plant species. In *Arabidopsis thaliana*, two proteins that interact with each other, named AtSUN1 and AtSUN2, have been identified. Immunolocalization using antibodies against AtSUN1 and AtSUN2 proteins revealed that they were associated with the nuclear envelope during meiotic prophase I. Analysis of the double mutant *Atsun1-1 Atsun2-2* has revealed severe meiotic defects, namely a delay in the progression of meiosis, absence of full synapsis, the presence of unresolved interlock-like structures, and a reduction in the mean cell chiasma frequency. We propose that in *Arabidopsis thaliana*, overlapping functions of SUN1 and SUN2 ensure normal meiotic recombination and synapsis.

Keywords: *Arabidopsis thaliana*, *Saccharomyces cerevisiae*, *Schizosaccharomyces pombe*, *Caenorhabditis elegans*, meiosis, nuclear envelope, SUN proteins.

INTRODUCTION

Meiosis is a highly conserved process that is essential for all sexually reproducing eukaryotes, and results in the production of haploid gametes or spores. In meiosis, a single round of DNA replication is followed by two rounds of chromosome segregation, resulting in halving of the chromosome number (Roeder, 1997). Subsequently, the diploid state is restored by fusion of the male and female gametes during fertilization. Homologous recombination is essential for establishing physical connections between homologous chromosomes in order that they may be segregated accurately during the first meiotic division (reviewed in Osman *et al.*, 2011). During the leptotene/zygotene transition of prophase I in many organisms, the telomeres cluster on the inner nuclear membrane of the nuclear envelope (NE), forming a so-called 'bouquet'. In many species, this persists until pachytene (Bass, 2003). The telomere attachment at the NE is adjacent to the microtubule organizing centres, i.e. the centrosome in animals and the spindle pole body in fungi (Scherthan, 2001). Using live-cell imaging of GFP-tagged Rap1, a telomere-binding protein, Trelles-Sticken *et al.* (2005) observed that addition of latrunculin B, which is known to prevent formation of actin cables, to a meiotic culture of wild-type *Saccharomyces cerevisiae* (budding yeast) prevented clustering of telomeres. Further work in budding yeast has revealed highly dynamic chromosome movements mediated by actin (Koszul *et al.*, 2008). These dramatic movements also cause protrusions in the NE, and were shown to be associated with the onset of zygotene, continuing throughout pachytene (Scherthan *et al.*, 2007; Koszul *et al.*, 2008). Actin cables were mostly observed close to the nucleus/cell periphery and the spindle pole body, and it was proposed that this may explain

the location of the bouquet in yeast (Koszul *et al.*, 2008). It has been suggested that these movements may create stirring motions that may bring homologous sequences into close proximity (Scherthan *et al.*, 2007). On the other hand, Koszul *et al.* (2008) postulated that these movements may prevent chromosome entanglements. More recent work in budding yeast has shown that sustained and rapid movement of chromosomes is necessary for effective pairing and meiotic progression (Brown *et al.*, 2011). In plants, there are no identified microtubule organizing centres, and consequently there is no obvious attachment site. Live-cell imaging of maize (*Zea mays*) meiocytes inside intact anthers demonstrated highly dynamic and complex actin- and tubulin-dependent chromosome movements during zygotene and pachytene (Sheehan and Pawlowski, 2009). Movements included rotational movements of the entire chromatin and movement of individual chromosome segments, which were mainly telomere-led. Chromosome movement coincided with deformations of the NE, as observed in budding yeast.

The link between the cytoskeleton and chromosome motility during meiosis was first discovered in *Schizosaccharomyces pombe* (Chikashige *et al.*, 2006), in which Bouquet 1 (Bqt1) and an interacting protein, Bouquet 2 (Bqt2), were found to prevent meiotic clustering and subsequent meiotic progression. It was proposed that these proteins interact to form a bridge between the telomeres and the NE by connecting Rap1, a telomere protein (Chikashige and Hiraoka, 2001), and Sad1, a component of the spindle pole body (Hagan and Yanagida, 1995). Bqt1 was shown to bind to the N-terminal region of Sad1. The C-terminal region contains a conserved domain, termed the SUN domain (for Sad1/UNC-84 homology; Malone *et al.*, 1999), and it was subsequently observed that proteins that tether other proteins to the NE also contain this characteristic domain (Tomita and Cooper, 2006). SUN domain proteins are membrane-integral components of the inner nuclear membrane with conserved structure and function (Starr, 2009). Their C-terminus, including the SUN domain, is located in the nuclear periplasm, where it interacts with the conserved KASH (Klarsicht/Anc/Syne homology) domain of a family of outer nuclear membrane proteins that in turn interact with elements of the cytoskeleton (Starr and Fridolfsson, 2010). The KASH protein structure includes a transmembrane domain and an N-terminus projecting into the cytoplasm. The periplasmic SUN/KASH interactions form the essential linkage that bridges the two membranes of the NE and forms nucleo-cytoskeletal linking complexes.

SUN domain proteins have been shown to play an important role in linking telomeres to the force-generating mechanism in the cytoplasm during meiosis in other organisms. For example, Schmitt *et al.* (2007) discovered that a rat SUN domain protein, SUN2, was localized to the attachment sites of meiotic telomeres at the NE. Electron microscopy showed that SUN2 is part of a membrane-spanning complex that connects attached telomeres to cytoplasmic structures, proposed to be the actin cytoskeleton. This study indicated that the mechanism for telomere attachment to the NE is conserved between eukaryotes. In mice, SUN1 deficiency prevents telomere attachment to the NE, and impairs pairing of homologous chromosomes, synapsis and recombination, resulting in complete sterility (Ding *et al.*, 2007). KASH5, a meiosis-specific outer nuclear membrane protein, was subsequently identified as the binding partner of SUN1, acting as a link to the microtubule-associated dynein–dynactin complex in the cytoplasm (Morimoto *et al.*, 2012; Horn *et al.*, 2013), although an association with chromosome movement has not been definitely confirmed. In a study to identify specific telomere-binding proteins, Shibukya *et al.* (2014) used a microarray based on ovarian material and identified a gene that they called *TERB1* (*CCDC79*). They suggest that this gene is involved in the assembly of the meiotic complex that is necessary for chromosome movements. This role has been confirmed by Daniel *et al.* (2014). The SUN1 protein of *Caenorhabditis elegans* has also been implicated in facilitating homologue pairing and restricting synapsis to regions of homologous pairing (Penkner *et al.*, 2007; Sato *et al.*, 2009), although, in this species, telomeres do not play a key role in meiotic chromosome motility, rather the chromosomes contain special homology recognition sites, known as pairing centres, that interact with the NE via association with one of a family of zinc-finger proteins (Phillips and Dernburg, 2006).

Putative SUN domain proteins have been identified in several plant species, with most studied possessing at least two proteins (Graumann *et al.*, 2010; Murphy *et al.*, 2010; Graumann and Evans, 2011; Oda and Fukuda, 2011). In addition to the classical C-terminal SUN domain proteins, evidence suggests the presence of a second group of SUN proteins in plants, in which the SUN domain is located in the centre of the protein (Murphy *et al.*, 2010), and a maize mid-SUN protein, ZmSUN3, has been hypothesized to play a role in meiosis (Murphy and Bass, 2012).

Using a combination of immunocytology and 3D microscopy, maize C-terminal SUN domain proteins were shown to form a dynamic belt-like structure during meiosis that exhibited stage-specific changes in morphology and included the telomere bouquet at zygotene (Murphy *et al.*, 2014). In various meiosis-specific chromosome segregation mutants, the belt was disrupted, providing further evidence for the role of SUN proteins in maize meiotic chromosome behaviour.

In *Arabidopsis thaliana*, recent attention has been paid to *AtSUN1* (At5g04990) and *AtSUN2* (At3g10730), which were previously identified as SUN domain homologues of the *C. elegans* SUN domain protein UNC-84 (Graumann *et al.*, 2010). AtSUN1 and AtSUN2 both have the

classical SUN protein structure, containing a highly conserved C-terminal SUN domain, a functional coiled-coil domain, a nuclear localization signal and an N-terminal transmembrane domain (Graumann *et al.*, 2010). They are both expressed in various tissues, including leaves and inflorescences, and are able to form homomeric and heteromeric complexes *in planta*. Similar to animals and yeast, the plant SUN proteins are also part of nucleo-cytoskeletal bridging complexes. Both AtSUN1 and AtSUN2 interact with outer nuclear membrane-localized WPP-domain interacting proteins 1–3 (AtWIP1–3) as well as SUN-Interacting NE 1 and 2 proteins (SINE 1 and 2), which are plant-specific KASH proteins (Zhou *et al.*, 2012, 2014; Zhou and Meier, 2013). These bridges are essential for linking the NE to the actin cytoskeleton. WIP1 interacts with WPP domain-interacting tail-anchored protein 1 (WIT1), which in turn associates with myosin XI-I (Tamura *et al.*, 2013), whilst SINE1 directly interacts with actin (Zhou *et al.*, 2014) Both the SUN/WIP/WIT/myosin XI-I/actin and SUN/SINE1/actin bridges control nuclear positioning and movement in Arabidopsis (Tamura *et al.*, 2013; Zhou *et al.*, 2014).

Here, we examine the localization of AtSUN1 and AtSUN2 in meiosis, and show that a double T-DNA insertional mutant, *Atsun1-1 Atsun2-2*, has meiotic defects, namely a delay in the progression of meiosis, absence of full synapsis and a reduction in the mean cell chiasma frequency. We propose that, in *Arabidopsis thaliana*, overlapping functions of SUN1 and SUN2 ensure normal meiotic recombination and synapsis.

RESULTS

Loss of AtSUN1 and AtSUN2 results in reduced fertility and meiotic defects

To investigate a potential meiotic role for AtSUN1 and AtSUN2, we analysed T-DNA insertional mutants of each gene: *Atsun1-1* (SAIL_84_G10), *Atsun2-1* (SALK_049398) and *Atsun2-2* (FLAG_026E12). Molecular characterization of *Atsun1-1* and *Atsun2-2* confirmed the presence of insertions 1955 and 1730 bp downstream from the ATG start codon, respectively (Figure S1a). In both cases, the insertion disrupts the SUN domain, and results in loss of cytoskeletal–nucleoskeletal bridging function (Zhou *et al.*, 2012, 2014). RT-PCR analysis confirmed the absence of any full-length transcript for both genes (Figure S1b). A second *AtSUN2* allele, *Atsun2-1*, contains an insertion 2056 bp downstream from the ATG start codon in the 3′ untranslated region of the gene, and has been reported to be a knockdown allele (Zhou *et al.*, 2012).

Homozygous *Atsun1-1*, *Atsun2-1 and Atsun2-2* single mutants were indistinguishable from wild-type (WT) plants. They exhibited normal vegetative growth, there was no obvious loss of fertility, and progression of the meiotic pathway appeared normal (Figures S2 and S3). To investigate the possibility of functional redundancy between the two genes, two double mutants were produced: *Atsun1-1 Atsun2-1* and *Atsun1-1 Atsun2-2*. In the case of *Atsun1-1 Atsun2-1*, vegetative growth and fertility were unaffected, and meiotic division and chiasma formation were normal (Figure S4). *Atsun1-1 Atsun2-2* also showed normal vegetative growth but had greatly reduced fertility, with a mean silique length of 6.8 ± 1.3 mm ($n = 20$) compared with 15.1 ± 0.5 mm ($n = 20$) in WT, while the mean number of seeds per silique was 2.1 ± 0.9 ($n = 20$) compared with 60.4 ± 2.5 ($n = 20$) in WT, representing a reduction of 96.5% in the double mutant.

Male meiosis in *Atsun1-1 Atsun2-2*

Spread preparations from pollen mother cells (PMCs) of *Atsun1-1 Atsun2-2* were examined using fluorescent microscopy to determine whether the reduced fertility phenotype was due to a defect in meiosis. Early prophase I in the double mutant did not appear to differ from WT, with chromosomes appearing as thin threads during leptotene (Figure 1a,i). In WT, pairing of homologous chromosomes is closely followed by synapsis, which begins in zygotene (Figure 1b) and progresses until pachytene, at which time homologues are connected along their entire length by the synaptonemal complex (SC) (Figure 1c). However, as meiosis progressed in the double mutant, only partially paired/synapsed cells were observed (Figure 1j,k), and no pachytene cells were seen. In every early *Atsun1-1 Atsun2-2* meiocyte that was partially synapsed, we identified one or more probable chromosome interlocks, which, in some cases, remained until metaphase I (Figure 2). During later stages, it became apparent that not all chromosome pairs were linked by chiasmata, the cytological manifestation of crossovers (COs). Instead of the five bivalents observed in WT metaphase I, *Atsun1-1 Atsun2-2* PMCs showed a mix of bivalents and univalents (Figure 1d,l). The presence of univalents led to chromosome mis-segregation at anaphase I, and unbalanced nuclei at the second division (Figure 1m–p).

Female meiosis in *Atsun1-1 Atsun2-2*

Spread preparations from megaspore mother cells (MMCs) of *Atsun1-1 Atsun2-2* were examined using fluorescence microscopy to determine whether female meiosis was also affected. We observed similar meiotic defects in MMCs ($n = 60$) (Figure 1q–t) to those observed in PMCs during male meiosis.

The duration of meiotic prophase I is extended in *Atsun1-1 Atsun2-2*

The cytological phenotype of partial synapsis in *Atsun1-1 Atsun2-2* may be evidence for a delay in prophase I of the meiotic pathway. We have investigated whether this is the case by performing a time-course experiment based on

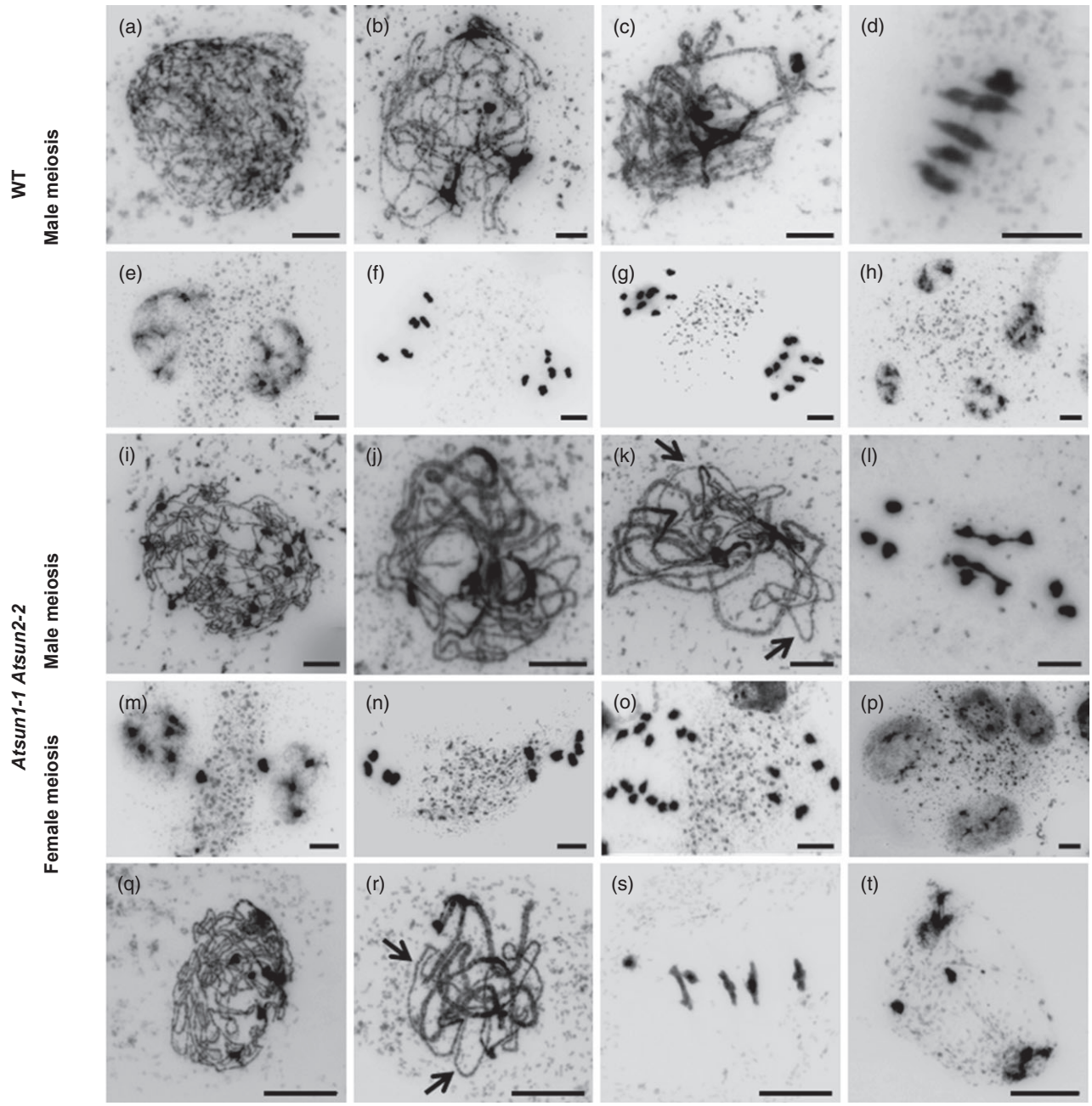

Figure 1. Loss of AtSUN1 and AtSUN2 results in defects in male and female meioses.
(a–h) Spread preparations from WT PMCs. (a) Leptotene. (b) Zygotene. (c) Pachytene with full synapsis. (d) Metaphase I with five ring bivalents. (e) Prophase II. (f) Metaphase II. (g) Anaphase II. (h) Tetrad.
(i–p) Spread preparations from *Atsun1-1 Atsun2-2* PMCs. (i) Leptotene. (j) Zytotene. (k) Pachytene with asynapsis in some regions (arrows). (l) Metaphase I with two rod bivalents and six univalents. (m) Prophase II with two chromosomes located in the organelle barrier. (n) Metaphase II with four chromosomes in one nucleus and six in the other. (o) Anaphase II with unbalanced nuclei. (p) Tetrad showing unequal nuclei.
(q–t) Spread preparations from *Atsun1-1 Atsun2-2* megaspore mother cells (MMCs). (q) Zygotene. (r) Pachytene with asynapsis in some regions (arrows). (s) Metaphase I with four bivalents and two univalents. (t) Telophase I with two lagging chromosomes.
Scale bars = 5 μm.

EdU (5-ethynyl-2′-deoxyuridine) pulse labelling of PMCs in S phase (Armstrong, 2013). This technique involves placing the cut ends of primary inflorescences in EdU solution for 2 h before transferring to water. The progression of prophase I may be monitored by sampling and fixing buds at 4 h intervals to create meiotic spreads of PMCs for EdU

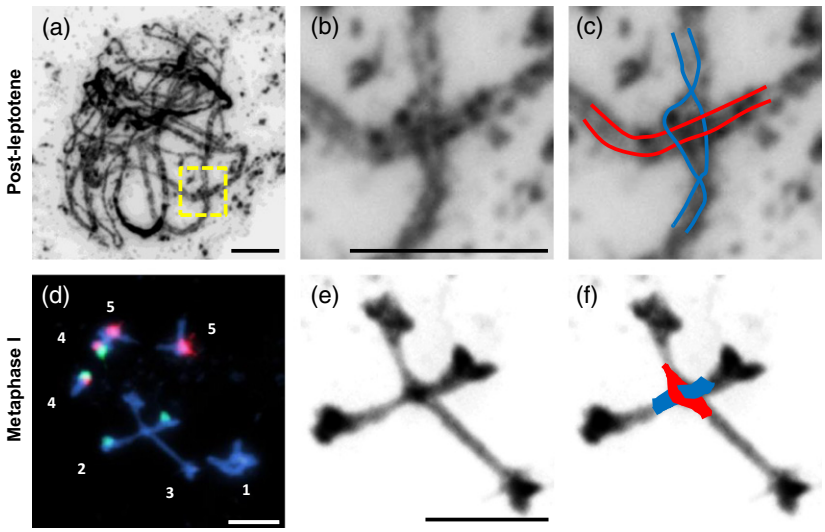

Figure 2. Interlock-like structures are frequent in *Atsun1-1 Atsun2-2*, remaining until metaphase I on some occasions.
(a–c) PMC at post-leptotene showing an interstitial interlock (a). (b) Detail of the interlock. A bivalent is trapped within a synapsing 'bubble'. (c) Schematic representation of the interlock.
(d–f) PMC at metaphase I with an interstitial interlock. (d) Individual chromosomes were identified by FISH using 5S (red) and 45S (green) rDNA as probes, and counterstained with DAPI (blue). The interlock was generated between chromosomes 2 and 3. (e) Detail of the interlock. (f) Schematic representation of the interlock.
Scale bars = 5 μm.

labelling. We considered the first labelling of a defined stage to indicate that the PMC had arrived at that stage, allowing us to assess the duration of individual stages of meiosis. In WT, labelled zygotene PMCs first appear at 16 h, and, by 24 h, labelling is observed in fully synapsed nuclei (Figure 3a–c). Labelled diplotene/diakinesis PMCs first appear at 32 h (Figure 3d–f), indicating that, in the WT, zygotene/pachytene occupies approximately 16 h of the total 36 h duration time from the meiotic S stage to the tetrad stage (Figure 3j). In *Atsun1-1 Atsun2-2*, labelled zygotene PMCs first appear at 16 h, as in WT. However, by 32 h, nuclei remain only partially synapsed (Figure 3g–i), no pachytene nuclei are ever observed, and labelled diplotene/diakinesis nuclei do not appear until 44 h. Thus, in the double mutant, early prophase I occupies approximately 28 h of the total duration time of 48 h from the meiotic S stage to the tetrad stage, indicating a delay of approximately 12 h in the progression of prophase I in *Atsun1-1 Atsun2-2* PMCs compared with WT (Figure 3j).

AtSUN1 and AtSUN2 are located at the NE of WT PMCs but are absent in *Atsun1-1 Atsun2-2*

We previously showed that AtSUN1 and AtSUN2 are widely expressed in somatic tissues and localize to the NE, particularly the inner nuclear membrane (Graumann *et al.*, 2010). In order to determine whether they also localize in meiotic cells, we performed immunolocalization of squash preparations of PMCs using antibodies raised against unique peptides within the AtSUN1 and AtSUN2 protein sequences (Graumann *et al.*, 2010). Figure 4(a–d) shows the distribution of antibody staining in WT PMCs at early prophase I, clearly indicating the localization of AtSUN1 (Figure 4a,b) and AtSUN2 (Figure 4c,d) at the NE. In contrast, immunolocalization of *Atsun1-1 Atsun2-2* PMCs at a similar stage confirmed the absence of AtSUN1 and AtSUN2 at the NE (Figure 4e–h), indicating that the meiotic abnormalities observed in this mutant result from loss of normal SUN protein localization and function.

Squash preparations are necessary to maintain the structure of the NE for immunolocalization with our antibodies. However, as background staining was observed using this technique, in order to confirm our observations on the meiotic localization of the two proteins, we used living anthers to perform confocal imaging of the expression of AtSUN1–GFP and AtSUN2–GFP under the control of their own promoters. In PMCs at meiotic interphase, as indicated by decondensed chromatin and a large nucleolus, both SUN proteins were localized evenly at the NE surrounding the chromatin (Figure 5a–d). For AtSUN1–GFP, the fluorescence at the NE in the interphase PMCs appeared weaker than the NE signal in the surrounding tapetal cells which may suggest lower expression of the protein (Figure 5a,b).

The localization of both SUN proteins changed dramatically during prophase I. As chromatin became more condensed, distinct foci containing AtSUN1–GFP and AtSUN2–GFP became visible (Figure 5e–h and Figure S5a–l). AtSUN1–GFP foci were mainly associated directly with the NE (Figure 5e,f), whereas AtSUN2–GFP foci were observed further from the NE but connected to it by what appeared to be an AtSUN2–GFP-stained membrane 'thread' (Figure 5g,h and Figure S5a–l). Usually only one focus was observed per NE. In addition to the foci, the NE-localized signal for both SUN proteins appeared polarized to one side of the NE during prophase I (Figure 5i–l and Figure S5a–l). At the end of the meiotic pathway, tetrads containing the four haploid products of meiosis were visible using the ethidium bromide counterstain (Figure 5m–p and Figure S5a–l). AtSUN2–GFP was present at the re-forming NEs around the tetrad chromatin (Figure 5o,p and Figure S5 m–t), where it appeared to localize much more strongly than AtSUN1–GFP did (Figure 5m,n and Figure S5 m–t).

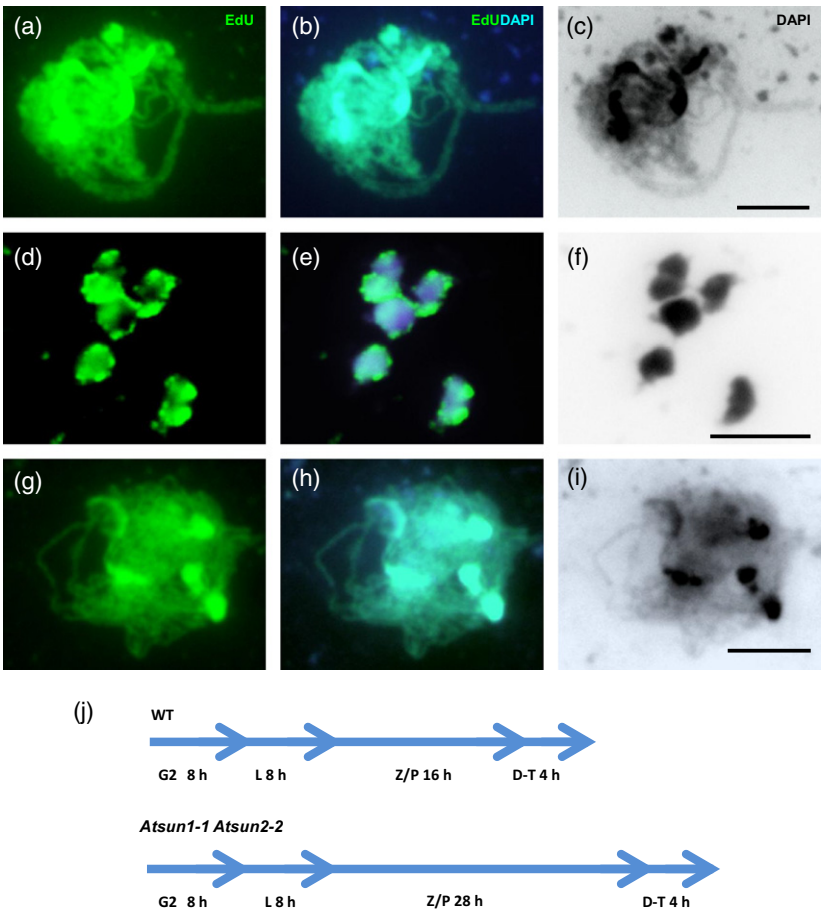

Figure 3. The duration of meiotic prophase I is extended in *Atsun1-1 Atsun2-2*.
(a–i) PMCs of WT and *Atsun1-1 Atsun2-2* were pulse-labelled with EdU (green) and viewed by immunofluorescence. DNA is stained with DAPI (blue). For clarity, grey-scale images of DAPI-stained DNA are also shown. (a–c) WT pachytene, 24 h; (d–f) WT diakinesis, 32 h; (g–i) *Atsun1-1 Atsun2-2* zygotene, 32 h. Scale bars = 5 μm.
(j) Time line comparing the duration of meiotic stages in WT and double mutant (j).

In addition, AtSUN1–GFP localization appeared more punctate (Figure 5m–p and Figure S5m–t).

Crossover frequency is reduced in *Atsun1-1 Atsun2-2*

The chiasma frequency for *Atsun1-1 Atsun2-2* was analysed in more detail using fluoresence *in situ* hybridization (FISH) in order to examine the behaviour of individual chromosomes (Figure 6). In *Arabidopsis thaliana*, 45S and 5S rDNA probes, combined with chromosome morphology, uniquely identify each of the chromosomes and chromosome arms (Sanchez-Moran *et al.*, 2002). The formation of meiotic COs/chiasmata is normally strictly regulated (Jones and Franklin, 2006), and this is reflected in the relatively narrow clustering of chiasma frequencies about the mean in WT lines. Thus the mean total chiasma frequency per cell in WT Columbia (Col-0, the *Atsun1-1* background) was 10.2 ± 0.14, with a range of 8–13 (n = 69) and that in WT Wassilewskija (Ws, the *Atsun2-2* background) was 9.85 ± 0.40, with a range of 8–12 (n = 56). The mean total chiasma frequency per cell in *Atsun1-1 Atsun2-2* was greatly reduced compared to either WT (3.32 ± 0.18, n = 128), and the range was much broader (0–9 chiasma per cell). Furthermore, chiasma loss in *Atsun1-1 Atsun2-2* was not restricted to any particular chromosome pair or pairs(s), but occurred across all members of the complement and affected both chromosome arms (Table 1).

Atsun1-1 Atsun2-2 PMCs have an altered distribution of centromeres, telomeres and 45S rDNA sequences

In order to examine *Atsun1-1 Atsun2-2* chromosome dynamics during pairing and synapsis, we performed FISH analysis of the distribution of centromeric regions (CENs), telomeric regions (TELs) and 45S rDNA (NORs) at various stages from meiotic interphase (G_2) to pachytene (Figure 7). As has been previously reported (Armstrong *et al.*, 2001), during G_2 in WT, up to 20 individual TEL sequences were observed, clustered around the periphery of the nucleolar region (Figure 7ai,ii), in addition to two CEN-associated signals resulting from the presence of an internal telomere repeat sequence on chromosome 1. In *A. thaliana*, pairing of homologous chromosomes is telomere-led, and this is reflected by a gradual reduction in the number of TEL signals (towards ten) by mid-leptotene (Figure 7aii,iii). As leptotene progresses, TELs no longer appear to be associated with the nucleolus, and, by zygotene, they are located at the periphery of the nucleus, loosely clustered in one hemisphere in a transient 'bouquet' formation (Figure 7aiv). During pachytene, TELs become more widely distributed,

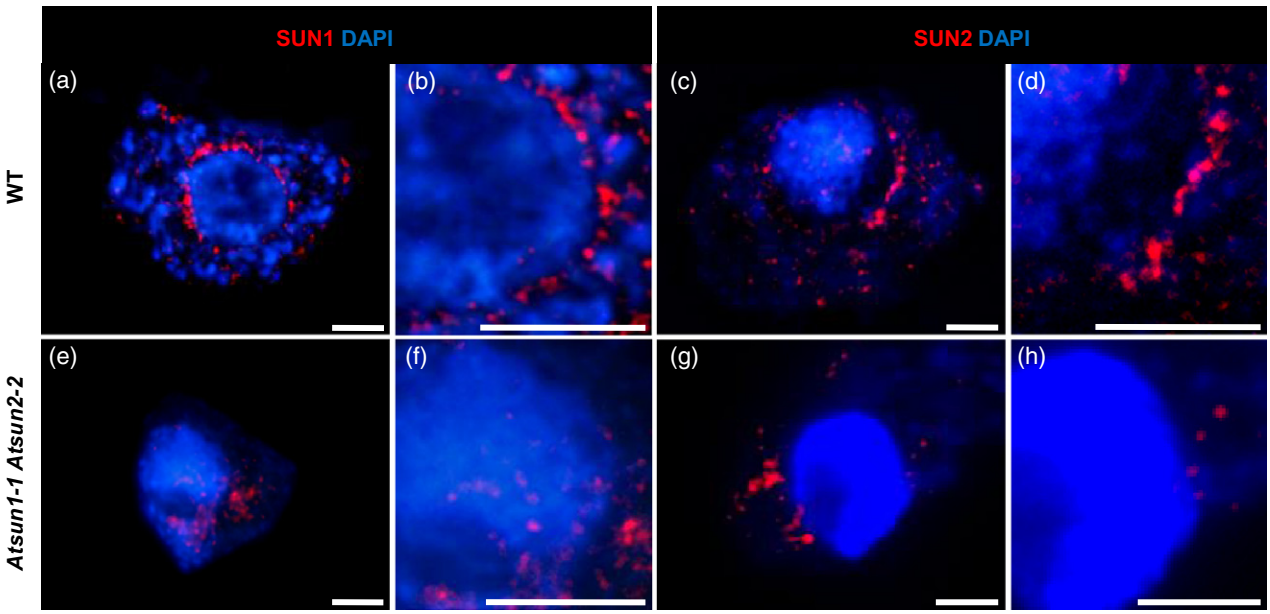

Figure 4. AtSUN1 and AtSUN2 are located around the NE during early prophase I in WT, but are not detected in *Atsun1-1 Atsun2-2*.
(a–d) Nuclear spreads of WT PMCs with AtSUN1 (a, b) and AtSUN2 (c, d) (red), detected by immunolocalization and counterstained using DAPI (blue). The images in (b) and (d) are details from (a) and (c), respectively. Both proteins are primarily located at the NE.
(e–h) Nuclear squashes of *Atsun1-1 Atsun2-2* PMCs with AtSUN1 (e,f) and AtSUN2 (g,h) (red), detected by immunolocalization and counterstained using DAPI (blue). The images in (f) and (h) are details from (e) and (g), respectively. The images illustrate the absence of AtSUN1 and AtSUN2 localization at the NE in the double mutant.
Scale bars = 5 μm.

but remain paired until diplotene (Figure 7av). CENs are dispersed peripherally in the nucleus during meiotic interphase and leptotene (Figure 7ai,ii), and undergo pairing later than TELs as indicated by a reduction in the number of distinct signals from ten to five by zygotene (Figure 7aiv) (Armstrong *et al.*, 2001). There is a tendency for CENs to cluster in one region of the nucleus during zygotene, but, by pachytene, they are more widely dispersed but remain paired (Figure 7aiv,v). In WT, the NORs, which are located on the short arms of chromosomes 2 and 4, tend to associate at the nucleolus during leptotene, concurrent with TEL pairing, and remain associated throughout zygotene and pachytene. This is reflected by a reduction in the number of NOR signals from four in G_2 to one by zygotene (Figure 7ai–v). Table 2 provides quantification of the observations for the various stages. In addition, in this context, the absence of association between the NORs in some cells reinforces the possibility that the bouquet is absent in the double mutant.

Typical zygotene and pachytene stages were not observed in *Atsun1-1 Atsun2-2*, so, for this analysis, cells were distinguished as being at G_2, leptotene or post-leptotene stages (Figure 7b). As in the WT, TELs in the double mutant were unpaired and clustered around the nucleolus at G_2 (Figure 7bi). As meiosis progressed, the number of TEL signals began to decrease, consistent with pairing, and the association with the nucleolus was lost, as in the WT (Figure 7bii). However, although telomere clusters were apparent, the characteristic transient bouquet was never observed (Figure 7biii,iv). Furthermore, in post-leptotene stages, some telomere association appeared to be lost, as indicated by the increase in the range of TEL signals at this stage compared to leptotene. The behaviour of the NORs also differed in the double mutant. Although, in some cells, NORs were observed to associate to create one signal during leptotene (Figure 7bii), a large proportion of post-leptotene cells exhibited non-associated NORs, as indicated by the presence of two signals (Figure 7biii). Even though full synapsis is not achieved in the double mutant, the CENs do eventually appear to pair (Figure 7biii–v). Table 3 provides quantification of the observations for the various stages. Interestingly, CENs even appear paired (five signals) in cells in which 45S rDNA regions are not associated and telomeres are unpaired. One possibility is that, in the absence of complete pairing/synapsis being achieved from the sub-telomeric ends, the centromeres take on a role in this process.

Immunolocalization of axis- and SC-associated proteins reveals extensive asynapsis in *Atsun1-1 Atsun2-2*

To further investigate the failure of *Atsun1-1 Atsun2-2* to complete synapsis, we performed immunolocalization of PMCs using antibodies against a range of chromosome axis- and SC-associated proteins: AtASY1, an axis-associated

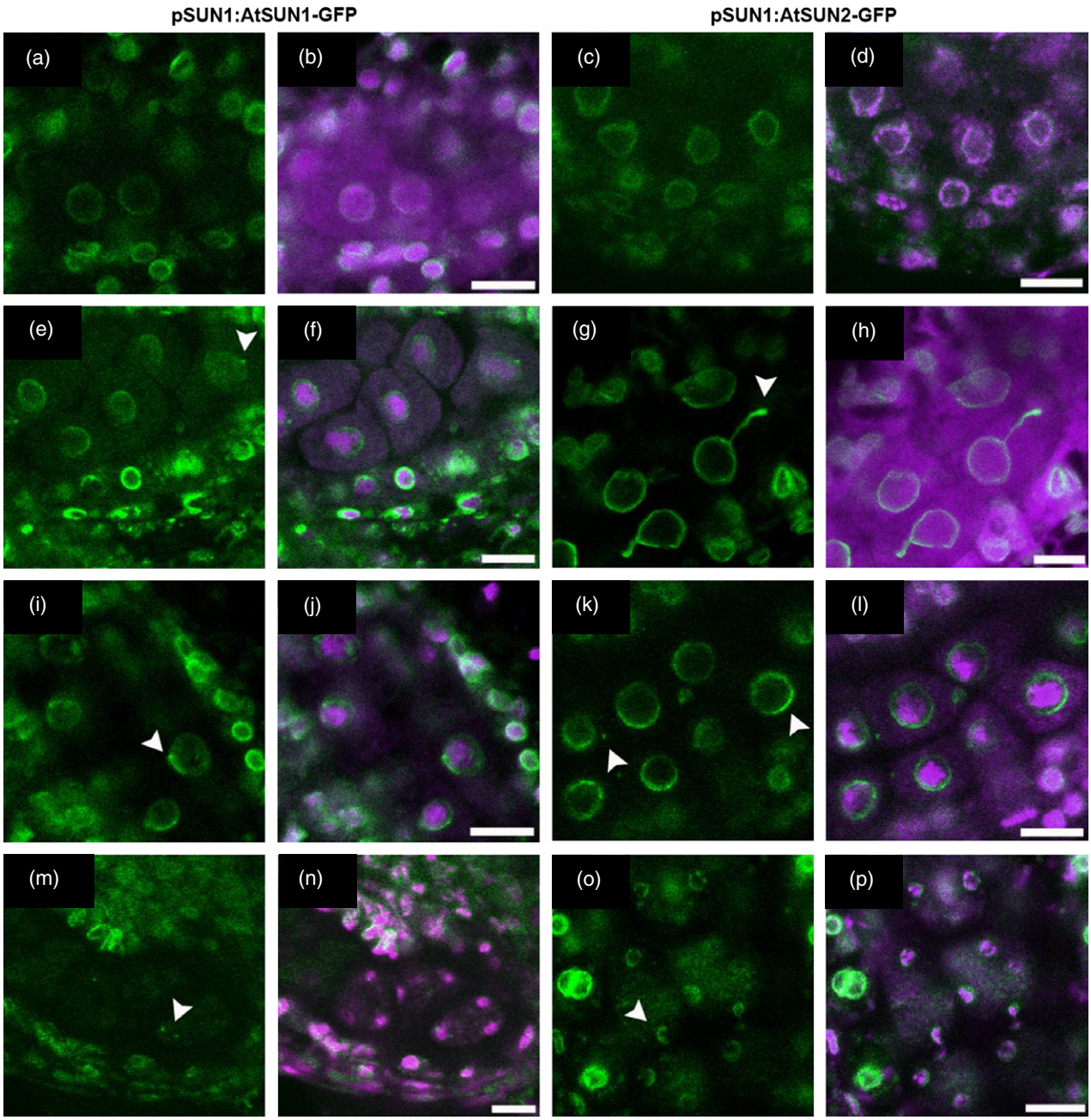

Figure 5. SUN protein localization in living Arabidopsis anthers.
AtSUN1 and AtSUN2 were expressed as GFP fusion proteins under the control of their native promoters in wild-type Arabidopsis. Their localization in PMCs, which appear as relatively large cells within each anther locule, is shown at various stages of meiosis: (a–d) interphase (G_2), (e–l) prophase I, (m–p) tetrads. GFP fluorescence appears green. Ethidium bromide-stained chromatin appears magenta. For each image, green and merged channels are shown. Arrowheads indicate key features described in main text. Scale bars = 10 μm.

HORMAD protein (Armstrong *et al.*, 2002), cohesin components AtSYN1 and AtSMC3 (Bai *et al.*, 1999; Lam *et al.*, 2005), and AtZYP1, the SC transverse filament protein (Higgins *et al.*, 2005). AtSYN1, AtSMC3 and AtASY1 labelling of the chromosome axes of *Atsun1-1 Atsun2-2* and the knockdown mutant *Atsun1-1 Atsun2-1* (which has some remaining AtSUN2 expression, Zhou *et al.*, 2012) was indistinguishable from that of the WT, suggesting that sister chromatid cohesion and axis formation take place as normal in the double mutants (Figure S6). In the *Atsun1-1 Atsun2-1* knockdown mutant, AtZYP1 loading also appeared to be normal (Figure S6). However, AtZYP1 loading in *Atsun1-1 Atsun2-2* was discontinuous, and did not extend along the full length of chromosomes, confirming the failure of this mutant to complete

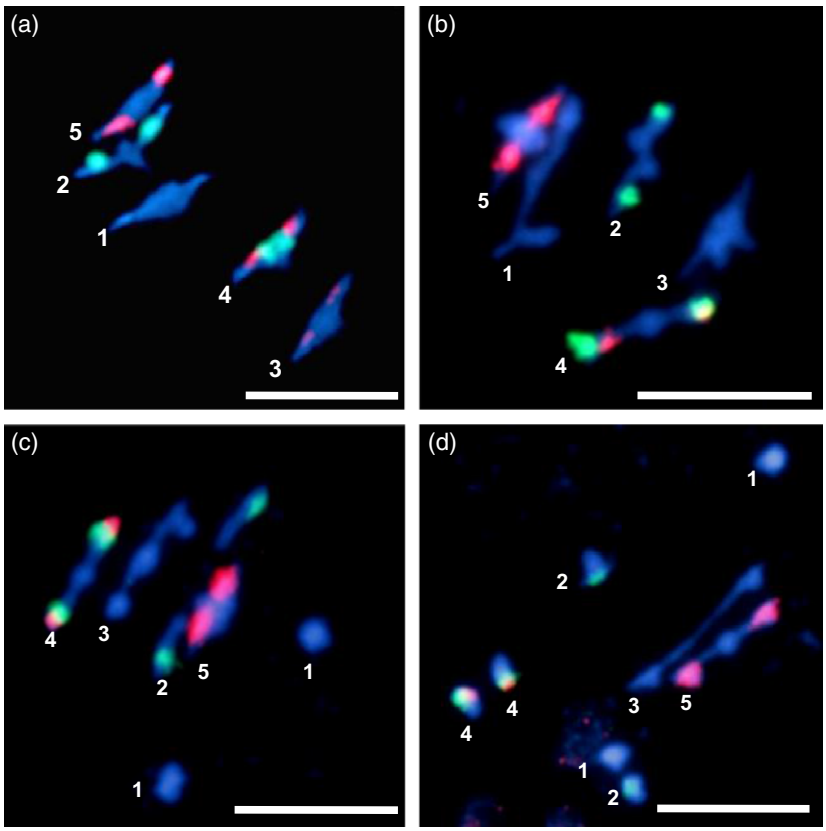

Figure 6. *Atsun1-1 Atsun2-2* shows a reduction in mean cell chiasma frequency.
Chromosomes were identified by FISH using 5S (red) and 45S (green) rDNA probes.
(a) Col-0 WT metaphase I showing five 'ring' bivalents with at least one chiasma in both arms.
(b–d) Representative images of metaphase I cells from *Atsun1-1 Atsun2-2*. In these examples, chromosome 3 is of Ws origin and lacks 5S rDNA sequences. (b) Five bivalents, seven chiasmata. (c) Four bivalents and two univalents, five chiasmata. (d) Two bivalents and six univalents, two chiasmata.
Scale bars = 5 μm.

Table 1 Mean chiasma frequencies per cell, per bivalent, and per bivalent arm

	Bivalent														
	1	2			3			4			5				
	S + L[a]	S	L	S + L	S	L	S + L	S	L	S + L	S	L	S + L	Total	*n*
Col-0	2.52	0.61	1.14	1.75	0.9	1.26	2.16	0.48	1.01	1.49	0.97	1.3	2.28	10.2 ± 0.14	69
Ws	2.42	0.78	1.14	1.92	0.71	1.07	1.78	0.64	1	1.64	0.85	1.21	2.07	9.85 ± 0.40	56
Atsun1-1 Atsun2-2	0.63	0.15	0.44	0.60	0.20	0.52	0.72	0.10	0.35	0.46	0.31	0.59	0.90	3.32 ± 0.18	128

S, short arm; L, long arm; *n*, number of cells analysed.
[a]It is not possible to distinguish the short and long arms in chromosome 1.

synapsis (Figure 8c,d and Figure S6). Measurements of SC length based on AtZYP1 staining show that *Atsun1-1 Atsun2-2* has a mean total synapsed length that is only approximately 50% of that of WT or *Atsun1-1 Atsun2-1*, and a maximum total synapsed length of approximately 73% (Table 4).

Loss of AtSUN1 and AtSUN2 affects localization of recombination pathway proteins

To further investigate the reduced CO frequency in *Atsun1-1 Atsun2-2*, we performed immunolocalization of proteins that function at various stages in the recombination pathway (Figure 9 and Table 5). We first examined the recombinases AtRAD51 and AtDMC1 (Doutriaux *et al.*, 1998). Although AtRAD51 foci are only an indirect measure of double-strand breaks (DSBs), the presence of approximately equal numbers in *Atsun1-1 Atsun2-2* and WT suggested that formation of DSBs was normal in the double mutant (Figure 9a,e). On the other hand, there was a significant decrease in the numbers of foci for AtDMC1, which is required for inter-homologue recombination (Couteau *et al.*, 1999), in *Atsun1-1 Atsun2-2*, to approximately 83% of the level in WT (Figure 9b,f). In *Atsun1-1 Atsun2-2*, we also observed a decrease in the number of foci for

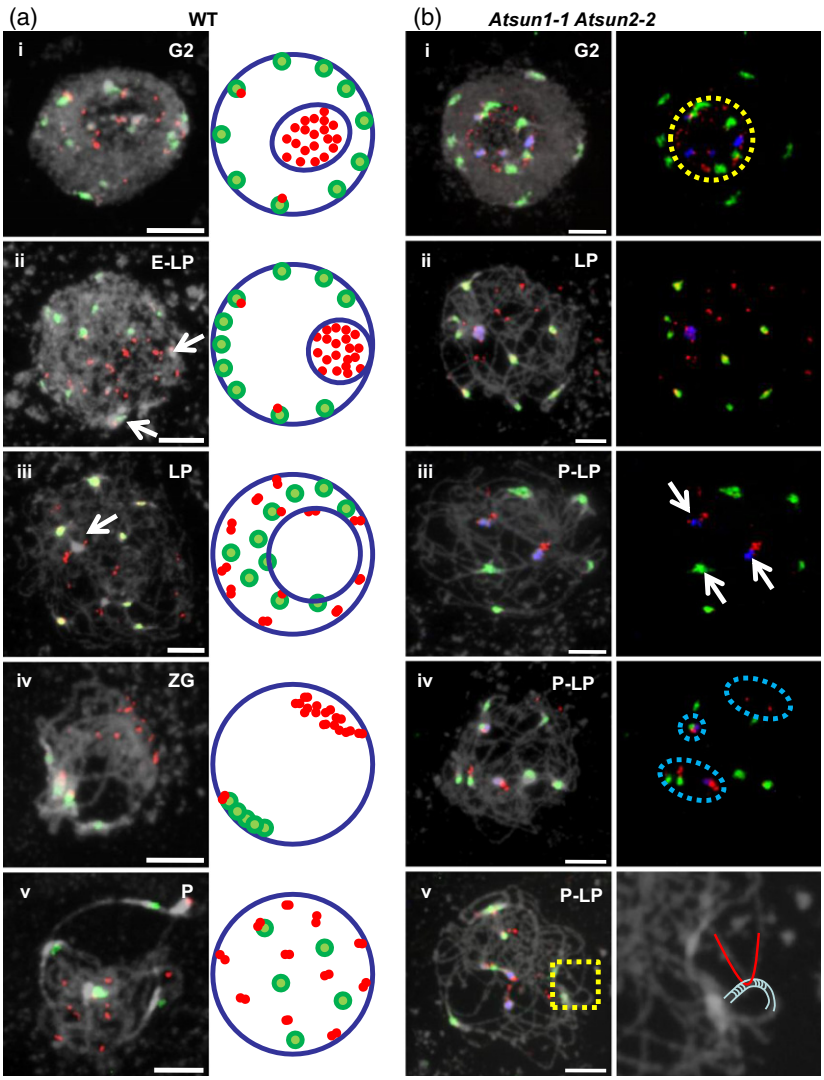

Figure 7. *Atsun1-1 Atsun2-2* shows altered distributions of centromeres, telomeres and NORs during prophase I.
(a) CENs (green) and TELs (red) in WT PMCs from G_2 to pachytene. NORs are indicated by arrows. A schematic representation has also been included. (i) G_2. (ii) Early leptotene (E-LP). (iii) Leptotene (LP). (iv) Zygotene (ZG). (v) Pachytene (P).
(b) CENs (green) and TELs (red) in *Atsun1-1 Atsun2-2* PMCs. NORs are labelled in blue. Images without DAPI counterstain have been included to allow better visualization of these regions. (i) G_2. The yellow dotted line represents the nucleolus. (ii) Leptotene (LP). (iii) Post-leptotene (P-LP). The arrows indicate two associated NORs and a paired centromere. (iv) P-LP. The dotted blue lines indicate aberrantly clustered TELs. (v) P-LP. The detail enclosed by the yellow dotted line has been enlarged in the adjacent image, and shows a probable interlock in which an unsynapsed chromosome (red) is trapped within an unsynapsed region of another bivalent (blue).
Scale bars = 5 μm.

AtMSH4, which is required for formation of normal levels of class I (interference-sensitive) COs (Higgins *et al.*, 2004) (Figure 9c,g) and in the number of AtMLH1 foci, which are thought to mark class I COs/chiasmata (Jackson *et al.*, 2006) (9d and 9h). The reductions in the numbers of AtMSH4 and AtMLH1 foci were even more marked than the decrease in AtDMC1 foci (to approximately 65% and approximately 30% of WT levels, respectively). Residual AtMLH1 foci were found to co-localize exclusively with the stretches of AtZYP1 present in *Atsun1-1 Atsun2-2*. Altogether, these results are consistent with the reduction in CO/chiasma frequency and SC length observed in the double mutant (Tables 1 and 4).

DISCUSSION

SUN/KASH proteins were originally identified on the basis of their role in nuclear migration and chromosome positioning, but several studies have shown that they also perform other functions, including involvement in centrosome attachment, formation of polarized nuclear shape, and chromosome organization and dynamics (Malone *et al.*, 2003; Chikashige *et al.*, 2007; Oda and Fukuda, 2011). The SUN domain is one of the most broadly conserved domains among NE proteins (Hiraoka and Dernburg, 2009), and the contribution of SUN domain proteins to meiotic chromosome dynamics has been demonstrated in several eukaryotic organisms (Fridkin *et al.*, 2009) but not previously in plants. Here, we provide cumulative evidence for the functional importance of AtSUN1 and AtSUN2 proteins in Arabidopsis meiosis.

SUN proteins are necessary for normal fertility

Whilst disruption of a single *SUN* gene usually results in an infertility phenotype in animals (Ding *et al.*, 2007), meiosis or fertility are not affected in single mutants for either *SUN1* or *SUN2* genes in *Arabidopsis thaliana*. We

Table 2 Number of FISH signals corresponding to centromeres, telomeres and 45S rDNA during prophase I in WT meiocytes

Number of centromeres	Mean number of telomeres[a]	45S rDNA[b]			Meiotic stage
10	18.35 ± 1.08[c]	A	0%		G_2
	(17–20)	NA	100%		
			20/20		
	14.16 ± 0.41	A	0%		E-LP
	(10–18)	NA	100%		
			25/25		
	11.21 ± 0.34	A	13.05%	10.81 ± 0.26	LP
	(10–16)		3/23	(10–14)	
		NA	86.95%	14.00 ± 1.15	
			20/23	(12–16)	
5	10.24 ± 0.08[d]	A	100%		ZG
	(10–14)		91/91		
		NA	0%		
	10.00	A	100%		P
	(10)		28/28		
		NA	0%		

[a]The values in parentheses represent the range.
[b]Percentage of 45S rDNA that is associated. In LP, 45S rDNA are associated in some cells. Means for the number of telomeres corresponding to each category (A and NA) are also shown.
[c]Telomeres are located around the nucleolus.
[d]Telomeres are clustered, forming the transient bouquet.
A, associated 45S rDNA; NA, non-associated 45S rDNA; E-LP, early leptotene; LP, leptotene; ZG, zygotene; P, pachytene.

therefore constructed lines with mutations in both genes (Figure S1a). The double mutant *Atsun1-1 Atsun2-1* appeared to have a normal phenotype (Figure S4). However, this was due to the mutation in the *Atsun2-1* allele being located in the downstream non-coding region of the gene, resulting in a truncated transcript that includes the entire protein coding region (Zhou *et al.*, 2012). In contrast, the double mutant *Atsun1-1 Atsun2-2*, in which both genes are disrupted in the SUN domain, showed a massive reduction in fertility (3.5% seed set) as a consequence of meiotic defects (Figure 1). Although Arabidopsis does not have a recombination checkpoint *per se*, and many recombination-defective mutants do manage to complete meiosis, albeit with varying degrees of success (Couteau *et al.*, 1999; Caryl *et al.*, 2000; Jackson *et al.*, 2006), mutants often exhibit a delay in the progression of prophase I, suggestive of the presence of a surveillance system (Higgins *et al.*, 2004, 2008 and Jackson *et al.*, 2006). Prophase I in *Atsun1-1 Atsun2-2* was delayed by approximately 12 h (Figure 3), but some cells, at least, were able to complete the division stages. Usually the result was unbalanced gametes due to mis-segregation, but occasionally, by chance, normal segregation produced viable gametes, thus explaining the residual fertility of this mutant.

Localization of AtSUN1 and AtSUN2 in PMCs suggests a chromatin-associated role

AtSUN1 and AtSUN2 localize at the NE of WT PMCs during prophase I but are absent in *Atsun1-1 Atsun2-2* (Figures 4 and 5). Two features of protein localization in WT are consistent with a role in chromosome attachment and movement. First, in some cells, AtSUN1–GFP and AtSUN2–GFP localization was polarized to one side of the NE in prophase I, in a pattern that bears a marked resemblance to the loose clustering of paired telomeres transiently observed at this stage (Figure 5i–l and Figure 7 aiv). Second, in addition to labelling the NE, AtSUN2–GFP was occasionally seen to form a single focus at some distance from the NE, which was connected to the NE by a thin, labelled membrane-like 'thread' (Figure 5g,h). Similar structures were observed during live imaging of prophase I chromosome movements in maize (Sheehan and Pawlowski, 2009) and in budding yeast, where it was proposed that they represent occasional distortions or ruptures in the sub-structure of the NE due to resistance to pulling forces exerted through the cytoskeleton (Koszul *et al.*, 2008; Koszul and Kleckner, 2009). Protrusions were telomere-led, and, although transient, were sometimes remarkably stable, persisting for more than 100 sec in some cases (Koszul *et al.*, 2008). It is possible that the AtSUN2–GFP-stained threads result from similar movements, and that the foci mark telomere attachment sites.

Telomere dynamics in the absence of AtSUN1 and AtSUN2 suggest failure to attach to the NE

Despite almost universal conservation of the bouquet arrangement in sexually reproducing organisms (Zickler and Kleckner, 1998), it appears to be not absolutely

Table 3 Number of FISH signals corresponding to centromeres, telomeres and 45S rDNA association during prophase I in *Atsun1-1 Atsun2-2* meiocytes

Number of centromeres	Mean number of telomeres[a]	45S rDNA[b]			Meiotic stage
10	17.37 ± 0.32[c] (14–20)	A	0%		G_2
		NA	100% 27/27		
	14.4 ± 2.03 (10–20)	A	0%		E-LP
		NA	100% 5/5		
9	12.00 ± 2.00 (10–14)	A	0%		
		NA	100% 2/2		
8	10.92 ± 0.28 (10–12)	A	38.46% 5/13	10.80 ± 0.48 (10–12)	LP
		NA	61.54% 8/13	11.00 ± 0.37 (10–12)	
7	11.69 ± 0.40 (10–16)	A	48.48% 16/33	11.12 ± 0.60 (10–16)	
		NA	51.52% 17/33	12.23 ± 0.51 (10–16)	
6	11.53 ± 0.27[d](10–18)	A	50.00% 30/60	11.20 ± 0.29 (10–18)	P-LP
		NA	50.00% 30/60	11.86 ± 0.44 (10–18)	
5	11.23 ± 0.21[d] (10–18)	A	39.70% 27/68	10.88 ± 0.30 (10–16)	
		NA	60.30% 41/68	11.46 ± 0.29 (10–18)	

A, associated 45S rDNA; NA, non-associated 45S rDNA; E-LP, early leptotene; LP, leptotene; P-LP, post-leptotene.
[a]The values in parentheses represent the range.
[b]Percentage of 45S rDNA that is associated. In LP and P-LP, NORs are associated in some cells. Means for the number of telomeres corresponding to each category (A and NA) are also shown.
[c]Telomeres are located around the nucleolus.
[d]The transient bouquet is absent.

required for either homologous pairing or synapsis (Harper *et al.*, 2004; Lee *et al.*, 2012). Indeed, in Arabidopsis, initial telomere-led pairing is clearly not dependent on bouquet formation, beginning while the telomeres are still associated with the nucleolus at the G_2 to leptotene transition (Figure 7a and Table 2) (Armstrong *et al.*, 2001; Roberts *et al.*, 2009). Only later in leptotene, subsequent to pairing, do the telomeres relocate to the nuclear periphery and then exhibit clustering to one side of the nucleus. However, although the true significance of the bouquet is still unknown, it is generally accepted that its formation is dependent on telomere attachment to the NE. Telomeres are known to be anchored to the NE by SUN proteins in evolutionarily distant organisms (Wilson and Dawson, 2011), indicating that this mechanism of attachment is highly conserved. There is now clear evidence from budding yeast that telomere-led chromosome movements resulting from NE attachment are responsible for promoting meiotic chromosome pairing, independently of bouquet formation (Lee *et al.*, 2012), and that the SUN domain itself is important for promoting the movements that control correct pairing and synapsis (Rao *et al.*, 2011). Telomere behaviour in *Atsun1-1 Atsun2-2* is consistent with a failure to anchor to the NE and form a stable attachment, and thus promote stable pairing (Figure 7b and Table 3). In early prophase I, chromosome dynamics appeared normal in *Atsun1-1 Atsun2-2*, with telomeres located around the nucleolus during G_2 and early leptotene, and pairing starting at the G_2 to leptotene transition as in WT. However, in later stages, the characteristic polarization to one side of the nucleus was never observed, and some early telomere pairing appeared to be lost. Examination of counterstained chromatin during these stages confirmed that chromosome pairing was not completed in the double mutant. The simplest explanation for these results is that, in the absence of AtSUN1 and AtSUN2, telomeres were unable to form a stable attachment at the NE, without which telomere-led pairing could not be maintained and extended. Despite the failure of *Atsun1-1 Atsun2-2* to complete pairing, centromeric regions did eventually pair, suggesting that, in the absence of stabilization of pairing from the telomeres, the centromeres are able to take over this

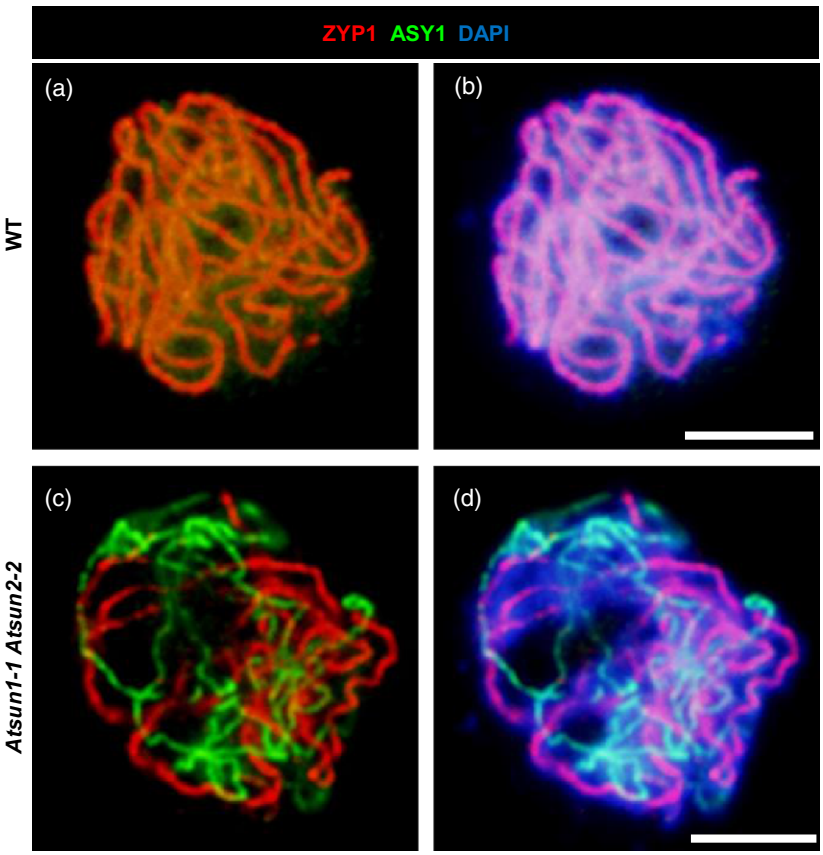

Figure 8. *Atsun1-1 Atsun2-2* fails to complete synapsis.
Nuclear spreads of PMCs with AtASY1 (green) and AtZYP1 (red) detected by immunolocalization and counterstained using DAPI (blue).
(a, b) WT PMCs. (a) Zygotene with partial synapsis. (b) Pachytene with full synapsis.
(c, d) *Atsun1-1 Atsun2-2* PMCs. (c) Post-leptotene, numerous stretches of AtZYP1-stained SC are visible. (d) Post-leptotene with more extensive but incomplete AtZYP1 labelling. AtASY1 signal remains on unsynapsed regions.
Scale bars = 5 μm.

role. This phenomenon has also been observed in some Arabidopsis asynaptic mutants that are defective in homologous recombination (Da Ines *et al.*, 2012). However, in both cases, it cannot be ruled out that these centromeric associations may be non-homologous in nature, at least in part.

Loss of AtSUN1 and AtSUN2 leads to severe meiotic defects

The central events of meiotic prophase I are pairing, recombination and synapsis, and, in Arabidopsis, as in most species, they are tightly integrated. Thus, failure of *Atsun1-1 Atsun2-2* to successfully complete homologous pairing had a profound effect on the outcome of meiosis in the mutant, resulting in extensive asynapsis, reduced CO/chiasma frequency and unresolved interlock-like structures, culminating in the mis-segregation of chromosomes at the division stages. Early steps in the meiotic pathway appeared normal. Loading of AtSYN1, AtSMC3 and AtASY1 onto the chromatin was indistinguishable from that in the WT, suggesting that sister chromatid cohesion and axis formation occurred normally (Figure S6). In addition, the number of AtRAD51 foci in *Atsun1-1 Atsun2-2* implied that formation of DSBs occurred at WT levels (Figure 9 and Table 5). Single-end invasions, and, by implication, homology searching, were also clearly initiated in *Atsun1-1 Atsun2-2*, as indicated by the presence of at least a degree of synapsis and CO formation (Figure 8 and Table 1). However, when the localization of AtDMC1, required for inter-homologue recombination, was examined, differences between *Atsun1-1 Atsun2-2* and WT began to emerge (Figure 9 and Table 5). The numbers of AtDMC1 foci in WT reach a maximum in the early part of leptotene, and remain at high levels in the majority of PMCs until the end of leptotene (Sanchez-Moran *et al.*, 2007). However, the peak number of AtDMC1 foci in the double mutant was reduced compared to WT. This may be

Table 4 Comparison between WT, *Atsun1-1 Atsun2-1* and *Atsun1-1 Atsun2-2* with respect to SC length

	WT	*Atsun1-1 Atsun2-1*	*Atsun1-1 Atsun2-2*
SC length (μm)	165.26 ± 4.79	158.23 ± 7.49	83.82 ± 4.89
Range (μm)	140.35–188.77	121.23–198.66	44.32–120.62
Percentage of synapsis	100%	100%	Mean: 50.71% Highest: 72.98%
Number of cells analysed	15	10	19

WT, wild-type; SC, synaptonemal complex.

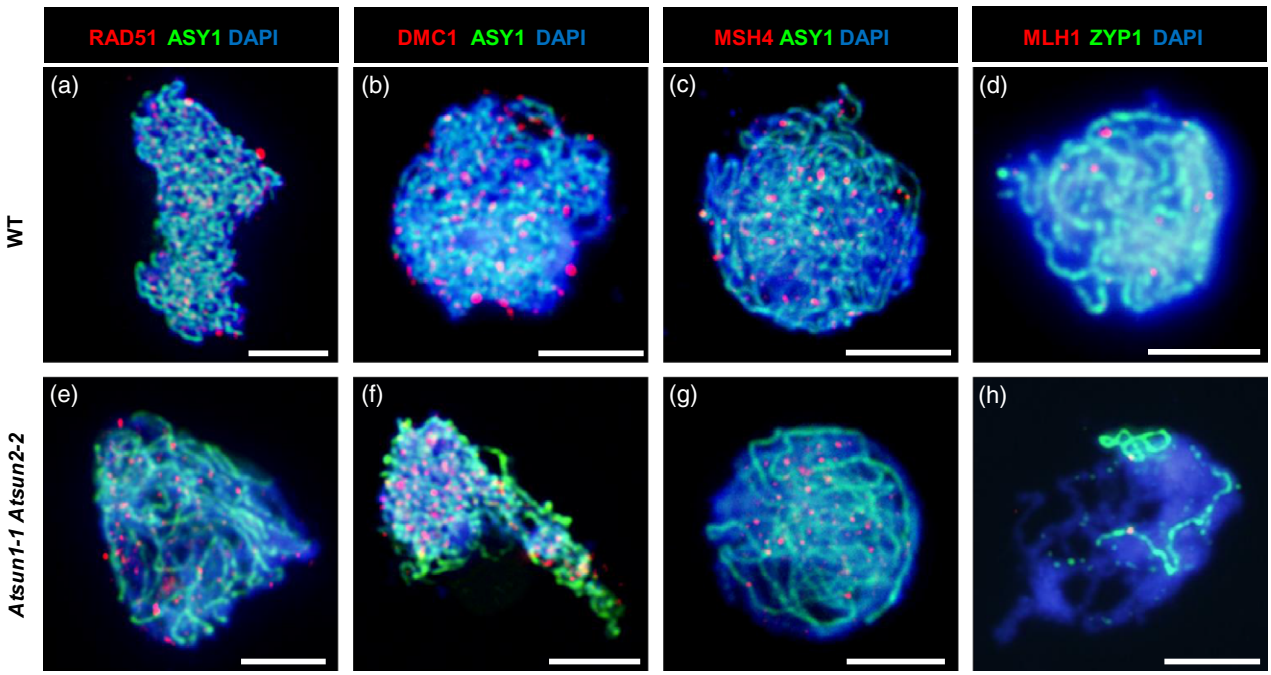

Figure 9. Loss of AtSUN1 and AtSUN2 affects AtDMC1, AtMSH4 and AtMLH1 foci, but AtRAD51 foci appear unaffected.
(a–d) Immunolocalization of nuclear spreads of WT PMCs with ASY1 (green) and AtRAD51 (a), AtDMC1 (b), AtMSH4 (c) and AtMLH1 (d) (red), counterstained using DAPI (blue).
(e–h) Immunolocalization of nuclear spreads of *Atsun1-1 Atsun2-2* PMCs with At ASY1 (green) and AtRAD51 (e), AtDMC1 (f), AtMSH4 (g) and AtMLH1 (h) (red), counterstained using DAPI (blue).
Scale bars = 5 μm.

due to a reduction in the absolute number of foci, or may simply reflect an alteration in the rate of turnover of foci. Either way, it implies that meiosis starts to deviate from normal sometime during mid- to late leptotene, which is broadly consistent with the stage at which paired telomeres move from their nucleolus-associated central location in the nucleus to the nuclear periphery (Roberts *et al.*, 2009). Taken together, these results suggest, that in the absence of telomere attachment at the NE to promote normal homologue pairing dynamics, formation of stable AtDMC1-associated recombination intermediates is perturbed. It should be pointed out that, despite the reduction in AtDMC1 foci in *Atsun1-1 Atsun2-2*, DSBs were repaired by AtRAD51, so no chromosomal fragmentation was observed.

Table 5 Comparison between WT and *Atsun1-1 Atsun2-2* with respect to the number of AtRAD51, AtDMC1, AtMSH4 and AtMLH1 foci

	WT	*Atsun1-1 Atsun2-2*	*P* value
AtRAD51	120.55 ± 2.44 (94–155) *n* = 38	121.00 ± 3.60 (91–153) *n* = 25	NS
AtDMC1	134.39 ± 3.82 (96–159) *n* = 25	111.48 ± 2.26 (83–138) *n* = 29	<0.001
AtMSH4	123.60 ± 3.49 (96–159) *n* = 25	80.00 ± 3.05 (54–124) *n* = 28	<0.001
AtMLH1	8.77 ± 0.42 (6–14) *n* = 28	2.71 ± 0.27 (0–7) *n* = 38	<0.001

The values in parentheses represent the range. *n*, number of cells analysed. Significance testing was performed using the Wilcoxon–Mann–Whitney test. NS, not significant.

The numbers of AtMSH4 and AtMLH1 foci were also significantly reduced in *Atsun1-1 Atsun2-2* (Figure 9 and Table 5). MSH4, together with its partner MSH5, are thought to form a sliding-clamp structure at progenitor double Holliday junctions to stabilize the formation of double Holliday junction intermediates (Snowden *et al.*, 2004, 2008). The probable reduction in the number of stable joint molecules in *Atsun1-1 Atsun2-2* therefore reduces the number of available sites for AtMSH4 localization, leading to a subsequent reduction in AtMLH1 foci and CO/chiasma frequency. Residual COs were able to form in those regions that do manage to pair and synapse, and it is notable that all remaining AtMLH1 foci in *Atsun1-1 Atsun2-2* are associated with stretches of SC (Figure 9). This also emphasizes the point that, in addition to its structural role within the SC, AtZYP1 plays an important role in CO formation and the prevention of non-allelic recombination

(Higgins *et al.*, 2005; Ferdous *et al.*, 2012). Thus, there is no evidence of ectopic recombination in *Atsun1-1 Atsun2-2*, unlike the situation in budding yeast, where abrogation of movement has been reported to slightly increase ectopic recombination (Conrad *et al.*, 2008). Although occasional metaphase I inter-bivalent connections were observed in *Atsun1-1 Atsun2-2*, they most likely resulted from a failure to resolve interlocked chromosomes rather than aberrant recombination (Figure 2). Unresolved interlocks, as a consequence of the absence of a removal mechanism normally provided by chromosome movements, have previously been discussed by Koszul and Kleckner (2009).

In conclusion, we suggest that, in the absence of AtSUN1 and AtSUN2, telomeres fail to anchor and form a stable attachment at the NE, without which telomere-led chromosome movements are not expected to occur. This in turn leads to impaired homologous pairing and synapsis, a delay in the progression of prophase I, reduced inter-homologue recombination and CO formation, and chromosome mis-segregation. This work indicates that the SUN proteins have a broadly conserved role, being key players in chromosome dynamics during meiosis. Further research is required to determine how these proteins facilitate coordination between cytoplasmic forces and the nucleus.

EXPERIMENTAL PROCEDURES

Plant material and DNA extraction

Arabidopsis thaliana ecotypes Columbia (Col-0) and Wassilewskija (Ws) were used for WT analysis. The T-DNA insertion lines SAIL_84_G10 (*Atsun1-1*) and SALK_048398 (*Atsun2-1*) were both in the Col-0 background, and were obtained from the Nottingham Arabidopsis Stock Centre (http://arabidopsis.info). FLAG_026E12 (*Atsun2-2*, Ws background) was obtained from the Versailles Arabidopsis Stock Centre (http://dbsgap.versailles.inra.fr/publiclines). Plants were grown, material was harvested and DNA was extracted as described previously by Higgins *et al.* (2004).

Plant genotyping and T-DNA insertion site mapping

The T-DNA insertion sites of *Atsun1-1*, *Atsun2-1* and *Atsun2-2* were amplified using the primers SUN1-F (5′-GGGGTTATTTC AATGACAATAACCGAG-3′) and SAIL-LB (5′-TTCATAACCAATCTCG ATACAC-3′), SUN2-1F (5′-CGTTGACAGAGAAAAGAACCG-3′) and LB2 (5′-GTGCTTTACGGCACCTCGAC-3′), and SUN2-2F (5′-GCTGT GACAATATGCATTGAGGAGG-3′) and FLAG-LB (5′-GCCAGGTGCC CACGGAATAGT-3′), respectively. The resulting PCR products were cloned into pDRIVE (Qiagen, http://www.qiagen.com), and sequenced by the Functional Genomics and Proteomics Unit (University of Birmingham, UK). The respective WT alleles were amplified using SUN1-F and SUN1-R (5′-GATGCGTTTTAAAGATT AACAGTATAAATTGG-3′), SUN2-1-F and SUN2-1-R (5′-GCTGTGTT GACTTGGAAGAGG-3′) and SUN2-2-F and SUN2-2-R (5′-GAC-TGAGTCTAGTTCACGGCC-3′).

Semi-quantitative RT-PCR for transcript expression

Total RNA was extracted from either 10-day-old seedlings or adult plant rosette leaves using a Nucleospin RNA extraction kit (ThermoFisher, http://www.thermofisher.com). Equal concentrations of total RNA were used as a template for cDNA synthesis, which was performed using a ProtoScript MuLV first-strand cDNA synthesis kit (NEB, https://www.neb.com). The coding sequences for *AtSUN1*, *AtSUN2* and the reference gene *Arabidopsis thaliana Protein Phosphatase 2A (Atpp2A)* were amplified from cDNA using Crimson Taq DNA polymerase (NEB) and the following primers: 5′-AT-GTCGGCATCAACGGTGTCG-3′ and 5′-TCGAGGTGAAGTCTAGCC-3′ for AtSUN1, 5′-ATGTCGGCGTCAACGGTGTC-3′ and 5′-TCAAGCAT GAGCAACAGAGAC-3′ for AtSUN2, and 5′-ATGTCTATGGTTGATGA GCC-3′ and 5′-GCTAGACATCATCACATTGTC-3′ for PP2A. Equal volumes of cDNA were used as templates, and equal volumes of PCR reaction mix were loaded onto agarose gels for electrophoresis and analysis.

Cytological procedures

Confocal imaging of anther meiocytes. Meiotic buds were removed from stable transformed Arabidopsis plants expressing either pAtSUN1:AtSUN1-GFP or pAtSUN2:AtSUN2-GFP (kindly donated by Hiroo Fukuda, Department of Biological Sciences, University of Tokyo) (Oda and Fukuda, 2011). Anthers were extracted and incubated for 15 min in ethidium bromide, followed by a 30 min incubation in perfluoromethylcyclohexane (Sigma, https://www.sigmaaldrich.com). Anthers were mounted in perfluoromethylcyclohexane on microscope slides, and imaged using an LSM 510 META (Zeiss, www.zeiss.co.uk). GFP was excited using a 488 nm laser, and fluorescence was captured between 505 and 530 nm; ethidium bromide was excited using a 543 nm laser, and fluorescence was captured using a 560 nm long-pass filter. Images were acquired using the LSM Image Browser (Zeiss).

Fixation, slide preparation and FISH. Preparations of PMCs and MMCs and the FISH technique were performed as previously described (Sanchez Moran *et al.*, 2001). The DNA probes used were pTa71 (for 45S rDNA, Gerlach and Bedbrook, 1979), pCT4.2 (for 5S rDNA, Campell *et al.*, 1992), pAL1 (for centromeres, Martinez-Zapater *et al.*, 1986) and pLT11 (for telomeres, Richards and Ausubel, 1988). Microscopy was performed using an Olympus, www.olympus.co.uk/ BX-60 microscope. Image capture was performed using an Olympus DP71 digital camera controlled by ANALYSIS SOFTWARE (Soft Imaging System, Olympus), and analysed and processed using ADOBE PHOTOSHOP CS4 software, www.adobe.com.

Protein immunolocalization. Preparation of PMCs for detection of AtSUN1 and AtSUN2 was performed by the squash technique as previously described (Oliver *et al.*, 2013) using the antibodies characterized in Graumann *et al.* (2010) diluted 1:100.

Preparation of PMCs for detection of the SC, cohesins and recombination-related proteins were performed by a spreading technique as previously described (Armstrong *et al.*, 2009). The primary antibodies used were anti-ASY1 (rat; 1:1000 dilution), anti-ZYP1 (rabbit; 1:500), anti-SYN1 (rabbit; 1:500), anti-SMC3 (rabbit; 1:500), anti-RAD51 (rabbit; 1:250), anti-DMC1 (rabbit; 1:250), anti-MSH4 (rabbit; 1:250) and anti-MLH1 (rabbit; 1:250) (Armstrong *et al.*, 2002; Mercier *et al.*, 2003; Higgins *et al.*, 2004, 2005; Tiang, 2010). Microscopy was performed as for FISH above.

Time-course analysis

The time-course analysis was based on the method described by Armstrong *et al.* (2003), and was performed using the thymidine analogue EdU and a Click-iT EDU HCS assay kit (HCS

NuclearMask™ Blue stain) (Invitrogen, http//www.lifetechnologies.com/) (Armstrong, 2013). Terminal inflorescences were cut under water and quickly transferred to a solution of EdU. The inflorescences were pulse-labelled for 2 h, transferred to water, then sampled and fixed at 4 h intervals (Armstrong, 2013). EdU labelling of PMCs was visualized using fluorescence microscopy of meiotic spreads after staining with a tagged antibody according to the kit instructions.

SC measurement

SC measurement was performed using ImageJ (http://rsbweb.nih.gov/ij/).

Accession numbers

The Arabidopsis Genome Initiative locus identifiers for AtSUN1, AtSUN2 and AtPP2A are At5g04990, At3g10730 and At1g13320, respectively.

ACKNOWLEDGEMENTS

We would like to thank Chris Franklin and Eugenio Sanchez-Moran for critical reading of the manuscript. Horticultural and technical support was provided by Steve Price and Karen Staples. D.E. and K.G. are grateful to the Leverhulme Trust for their support under grant number F/00 382H. K.G. is a Leverhulme Trust Early Career Fellow (ECF-2012-006). Research in the Universidad Complutense de Madrid and University of Birmingham laboratories has received funding from the European Community's Seventh Framework Programme FP7/2007–2013 under grant agreement number KBBE-2009-222883. The University of Birmingham laboratory has also received support from the Biotechology and Biological Sciences Research Council (BBSRC).

SUPPORTING INFORMATION

Additional Supporting Information may be found in the online version of this article.

Figure S1. Schematic representation of *Atsun1-1*, *Atsun2-1* and *Atsun2-2* T-DNA insertions in SUN genes, and RT-PCR analysis of *Atsun1-1 Atsun2-2*.

Figure S2. Cytological characterization of meiosis in *Atsun1-1* PMCs.

Figure S3. Cytological characterization of meiosis in *Atsun2-2* PMCs.

Figure S4. Cytological characterization of meiosis in *Atsun1-1 Atsun2-1* PMCs.

Figure S5. Localization of AtSUN1–GFP and AtSUN2–GFP in PMCs.

Figure S6. The chromosome axes appear normal in *Atsun1-1 Atsun2-1* and *Atsun1-1 Atsun2-2*.

REFERENCES

Armstrong, S.J. (2013). A time course for the analysis of meiotic progression in Arabidopsis thaliana. *Methods Mol Biol*, **990**, 119–123.

Armstrong, S.J., Franklin, F.C.H. and Jones, G.H. (2001) Nucleolus-associated telomere clustering and pairing precede meiotic chromosome synapsis in *Arabidopsis thaliana*. *J. Cell Sci.* **114**, 4207–4217.

Armstrong, S.J., Franklin, F.C.H. and Jones, G.H. (2003) A meiotic time course for *Arabidopsis thaliana*. *Sexual Plant Reprod* **16**, 141–149.

Armstrong, S.J., Caryl, A.P., Jones, G.H. and Franklin, F.C.H. (2002) Asy1, a protein required for meiotic chromosome synapsis, localizes to axis-associated chromatin in Arabidopsis and Brassica. *J. Cell Sci.* **115**, 3645–3655.

Armstrong, S., Sanchez-Moran, E. and Franklin, F.C.H. (2009). Cytological analysis of *Arabidopsis thaliana* meiotic chromosomes. In *Meiosis* (Keeney, S. ed): Humana Press, pp. 131–145.

Bai, X., Peirson, B.N., Dong, F., Xue, C. and Makaroff, C.A. (1999) Isolation and characterization of SYN1, a RAD21-like gene essential for meiosis in arabidopsis. *Plant Cell*, **11**, 417–430.

Bass, H.W. (2003) Telomere dynamics unique to meiotic prophase: formation and significance of the bouquet. *Cell. Mol. Life Sci.* **60**, 2319–2324.

Brown, M.S., Zanders, S. and Alani, E. (2011) Sustained and rapid chromosome movements are critical for chromosome pairing and meiotic progression in budding yeast. *Genetics*, **188**, 21–32.

Campell, B.R., Song, Y., Posch, T.E., Cullis, C.A. and Town, C.D. (1992) Sequence and organization of 5S ribosomal RNA-encoding genes of *Arabidopsis thaliana*. *Gene*, **112**, 225–228.

Caryl, A.P., Armstrong, S.J., Jones, G.H. and Franklin, F.C.H. (2000) A homologue of the yeast HOP1 gene is inactivated in the Arabidopsis meiotic mutant asy1. *Chromosoma*, **109**, 62–71.

Chikashige, Y. and Hiraoka, Y. (2001) Telomere binding of the Rap1 protein is required for meiosis in fission yeast. *Curr. Biol.* **11**, 1618–1623.

Chikashige, Y., Tsutsumi, C., Yamane, M., Okamasa, K., Haraguchi, T. and Hiraoka, Y. (2006) Meiotic proteins Bqt1 and Bqt2 tether telomeres to form the bouquet arrangement of chromosomes. *Cell*, **125**, 59–69.

Chikashige, Y., Haraguchi, T. and Hiraoka, Y. (2007) Another way to move chromosomes. *Chromosoma*, **116**, 497–505.

Conrad, M.N., Lee, C.-Y., Chao, G., Shinohara, M., Kosaka, H., Shinohara, A., Conchello, J.A. and Dresser, M.E. (2008) Rapid telomere movement in meiotic prophase is promoted by NDJ1, MPS3, and CSM4 and is modulated by recombination. *Cell*, **133**, 1175–1187.

Couteau, F., Belzile, F., Horlow, C., Grandjean, O., Vezon, D. and Doutriaux, M.-P. (1999) Random chromosome segregation without meiotic arrest in both male and female meiocytes of a Dmc1 mutant of *Arabidopsis*. *Plant Cell*, **11**, 1623–1634.

Da Ines, O., Abe, K., Goubely, C., Gallego, M.E. and White, C.I. (2012) Differing requirements for RAD51 and DMC1 in meiotic pairing of centromeres and chromosome arms in *Arabidopsis thaliana*. *PLoS Genet.* **8**, e1002636.

Daniel, K., Tränkner, D., Wojtasz, L., Shibuya, H., Watanabe, Y., Alsheimer, M. and Tóth, A. (2014) Mouse CCDC79 (TERB1) is a meiosis–specific telomere associated protein. *BMC Cell Biol.* **15**, 17.

Ding, X., Xu, R., Yu, J., Xu, T., Zhuang, Y. and Han, M. (2007) SUN1 is required for telomere attachment to nuclear envelope and gametogenesis in mice. *Dev. Cell*, **12**, 863–872.

Doutriaux, M.P., Couteau, F., Bergounioux, C. and White, C. (1998) Isolation and characterisation of the RAD51 and DMC1 homologs from *Arabidopsis thaliana*. *Mol. Gen. Genet.* **257**, 283–291.

Ferdous, M., Higgins, J.D., Osman, K. *et al.* (2012) Inter-homolog crossing-over and synapsis in *Arabidopsis* meiosis are dependent on the chromosome axis protein AtASY3. *PLoS Genet.* **8**, e1002507.

Fridkin, A., Penkner, A., Jantsch, V. and Gruenbaum, Y. (2009) SUN-domain and KASH-domain proteins during development, meiosis and disease. *Cell. Mol. Life Sci.* **66**, 1518–1533.

Gerlach, W.L. and Bedbrook, J.R. (1979) Cloning and characterization of ribosomal RNA genes from wheat and barley. *Nucleic Acids Res.* **7**, 1869–1885.

Graumann, K. and Evans, D.E. (2011) Nuclear envelope dynamics during plant cell division suggest common mechanisms between kingdoms. *Biochem. J.* **435**, 661–667.

Graumann, K., Runions, J. and Evans, D.E. (2010) Characterization of SUN-domain proteins at the higher plant nuclear envelope. *Plant J.* **61**, 134–144.

Hagan, I. and Yanagida, M. (1995) The product of the spindle formation gene sad1+ associates with the fission yeast spindle pole body and is essential for viability. *J. Cell Biol.* **129**, 1033–1047.

Harper, L., Golubovskaya, I. and Cande, W.Z. (2004) A bouquet of chromosomes. *J. Cell Sci.* **117**, 4025–4032.

Higgins, J.D., Armstrong, S.J., Franklin, F.C.H. and Jones, G.H. (2004) The Arabidopsis MutS homolog AtMSH4 functions at an early step in recom-

bination: evidence for two classes of recombination in Arabidopsis. *Genes Dev.* **18**, 2557–2570.

Higgins, J.D., Sanchez-Moran, E., Armstrong, S.J., Jones, G.H. and Franklin, F.C.H. (2005) The Arabidopsis synaptonemal complex protein ZYP1 is required for chromosome synapsis and normal fidelity of crossing over. *Genes Dev.* **19**, 2488–2500.

Higgins, J.D., Vignard, J., Mercier, R., Pugh, A.G., Franklin, F.C.H. and Jones, G.H. (2008) AtMSH5 partners AtMSH4 in the class I meiotic crossover pathway in *Arabidopsis thaliana*, but is not required for synapsis. *Plant J.* **55**, 28–39.

Hiraoka, Y. and Dernburg, A.F. (2009) The SUN rises on meiotic chromosome dynamics. *Dev. Cell*, **17**, 598–605.

Horn, H.F., Kim, D.I., Wright, G.D., Wong, E.S.M., Stewart, C.L., Burke, B. and Roux, K.J. (2013) A mammalian KASH domain protein coupling meiotic chromosomes to the cytoskeleton. *J. Cell Biol.* **202**, 1023–1039.

Jackson, N., Sanchez-Moran, E., Buckling, E., Armstrong, S.J., Jones, G.H. and Franklin, F.C.H. (2006) Reduced meiotic crossovers and delayed prophase I progression in AtMLH3-deficient Arabidopsis. *EMBO J.* **25**, 1315–1323.

Jones, G.H. and Franklin, F.C.H. (2006) Meiotic crossing-over: obligation and interference. *Cell*, **126**, 246–248.

Koszul, R. and Kleckner, N. (2009) Dynamic chromosome movements during meiosis: a way to eliminate unwanted connections? *Trends Cell Biol.* **19**, 716–724.

Koszul, R., Kim, K.P., Prentiss, M., Kleckner, N. and Kameoka, S. (2008) Meiotic chromosomes move by linkage to dynamic actin cables with transduction of force through the nuclear envelope. *Cell*, **133**, 1188–1201.

Lam, W.S., Yang, X. and Makaroff, C.A. (2005) Characterization of *Arabidopsis thaliana* SMC1 and SMC3: evidence that AtSMC3 may function beyond chromosome cohesion. *J. Cell Sci.* **118**, 3037–3048.

Lee, C.-Y., Conrad, M.N. and Dresser, M.E. (2012) Meiotic chromosome pairing is promoted by telomere-led chromosome movements independent of bouquet formation. *PLoS Genet.* **8**, e1002730.

Malone, C.J., Fixsen, W.D., Horvitz, H.R. and Han, M. (1999) UNC-84 localizes to the nuclear envelope and is required for nuclear migration and anchoring during *C. elegans* development. *Development*, **126**, 3171–3181.

Malone, C.J., Misner, L., Le Bot, N., Tsai, M.-C., Campbell, J.M., Ahringer, J. and White, J.G. (2003) The *C. elegans* hook protein, ZYG-12, mediates the essential attachment between the centrosome and nucleus. *Cell*, **115**, 825–836.

Martinez-Zapater, J., Estelle, M. and Somerville, C. (1986) A highly repeated DNA sequence in *Arabidopsis thaliana*. *Mol. Gen. Genet.* **204**, 417–423.

Mercier, R., Armstrong, S.J., Horlow, C., Jackson, N.P., Makaroff, C.A., Vezon, D., Pelletier, G., Jones, G.H. and Franklin, F.C.H. (2003) The meiotic protein SWI1 is required for axial element formation and recombination initiation in Arabidopsis. *Development*, **130**, 3309–3318.

Morimoto, A., Shibuya, H., Zhu, X., Kim, J., Ishiguro, K.-I., Han, M. and Watanabe, Y. (2012) A conserved KASH domain protein associates with telomeres, SUN1, and dynactin during mammalian meiosis. *J. Cell Biol.* **198**, 165–172.

Murphy, S. and Bass, H. (2012) The maize (Zea mays) desynaptic (dy) mutation defines a pathway for meiotic chromosome segregation, linking nuclear morphology, telomere distribution and synapsis. *J. Cell Sci.* **1**, 3681–3690.

Murphy, S., Simmons, C. and Bass, H. (2010) Structure and expression of the maize (*Zea mays* L.) SUN-domain protein gene family: evidence for the existence of two divergent classes of SUN proteins in plants. *BMC Plant Biol.* **10**, 269.

Murphy, S., Gumber, H.K., Mao, Y. and Bass, H. (2014) A dynamic meiotic SUN belt includes the zygotene-stage telomere bouquet and is disrupted in chromosome segregation mutants of maize (Zea mays L.). *Front Plant Sci.* **5**, 314.

Oda, Y. and Fukuda, H. (2011) Dynamics of Arabidopsis SUN proteins during mitosis and their involvement in nuclear shaping. *Plant J.* **66**, 629–641.

Oliver, C., Pradillo, M., Corredor, E. and Cuñado, N. (2013) The dynamics of histone H3 modifications is species-specific in plant meiosis. *Planta*, **238**, 23–33.

Osman, K., Higgins, J.D., Sanchez-Moran, E., Armstrong, S.J. and Franklin, F.C.H. (2011) Pathways to meiotic recombination in *Arabidopsis thaliana*. *New Phytol.* **190**, 523–544.

Penkner, A., Tang, L., Novatchkova, M., Ladurner, M., Fridkin, A., Gruenbaum, Y., Schweizer, D., Loidl, J. and Jantsch, V. (2007) The nuclear envelope protein Matefin/SUN-1 is required for homologous pairing in *C. elegans* meiosis. *Dev. Cell*, **12**, 873–885.

Phillips, C.M. and Dernburg, A.F. (2006) A family of zinc-finger proteins is required for chromosome-specific pairing and synapsis during meiosis in *C. elegans*. *Dev. Cell*, **11**, 817–829.

Rao, H.B.D., Shinohara, M. and Shinohara, A. (2011) Mps3 SUN domain is important for chromosome motion and juxtaposition of homologous chromosomes during meiosis. *Genes Cells*, **16**, 1081–1096.

Richards, E.J. and Ausubel, F.M. (1988) Isolation of a higher eukaryotic telomere from *Arabidopsis thaliana*. *Cell*, **53**, 127–136.

Roberts, N.Y., Osman, K. and Armstrong, S.J. (2009) Telomere distribution and dynamics in somatic and meiotic nuclei of *Arabidopsis thaliana*. *Cytogenet. Genome Res.* **124**, 193–201.

Roeder, G.S. (1997) Meiotic chromosomes: it takes two to tango. *Genes Dev.* **11**, 2600–2621.

Sanchez Moran, E., Armstrong, S.J., Santos, J.L., Franklin, F.C. and Jones, G.H. (2001) Chiasma formation in *Arabidopsis thaliana* accession Wassileskija and in two meiotic mutants. *Chromosome Res.* **9**, 121–128.

Sanchez-Moran, E., Armstrong, S.J., Santos, J.L., Franklin, F.C.H. and Jones, G.H. (2002) Variation in Chiasma frequency among eight accessions of *Arabidopsis thaliana*. *Genetics*, **162**, 1415–1422.

Sanchez-Moran, E., Santos, J.-L., Jones, G.H. and Franklin, F.C.H. (2007) ASY1 mediates AtDMC1-dependent interhomolog recombination during meiosis in Arabidopsis. *Genes Dev.* **21**, 2220–2233.

Sato, A., Isaac, B., Phillips, C.M., Rillo, R., Carlton, P.M., Wynne, D.J., Kasad, R.A. and Dernburg, A.F. (2009) Cytoskeletal forces span the nuclear envelope to coordinate meiotic chromosome pairing and synapsis. *Cell*, **139**, 907–919.

Scherthan, H. (2001) A bouquet makes ends meet. *Nat. Rev. Mol. Cell Biol.* **2**, 621–627.

Scherthan, H., Wang, H., Adelfalk, C., White, E.J., Cowan, C., Cande, W.Z. and Kaback, D.B. (2007) Chromosome mobility during meiotic prophase in *Saccharomyces cerevisiae*. *Proc. Natl Acad. Sci. USA*, **104**, 16934–16939.

Schmitt, J., Benavente, R., Hodzic, D., Höög, C., Stewart, C.L. and Alsheimer, M. (2007) Transmembrane protein Sun2 is involved in tethering mammalian meiotic telomeres to the nuclear envelope. *Proc. Natl Acad. Sci. USA*, **104**, 7426–7431.

Sheehan, M.J. and Pawlowski, W.P. (2009) Live imaging of rapid chromosome movements in meiotic prophase I in maize. *Proc. Natl Acad. Sci. USA*, **106**, 20989–20994.

Shibukya, H., Ishiguro, K. and Watanabe, Y. (2014) The TRF1-binding protein TERB1 promotes chromosome movement and telomere rigidity in meiosis. *Nat. Cell Biol.* **16**, 145–158.

Snowden, T., Acharya, S., Butz, C., Berardini, M. and Fishel, R. (2004) hMSH4-hMSH5 recognizes Holliday junctions and forms a meiosis-specific sliding clamp that embraces homologous chromosomes. *Mol. Cell*, **15**, 437–451.

Snowden, T., Shim, K.-S., Schmutte, C., Acharya, S. and Fishel, R. (2008) hMSH4-hMSH5 adenosine nucleotide processing and interactions with homologous recombination machinery. *J. Biol. Chem.* **283**, 145–154.

Starr, D.A. (2009) A nuclear-envelope bridge positions nuclei and moves chromosomes. *J. Cell Sci.* **122**, 577–586.

Starr, D.A. and Fridolfsson, H.N. (2010) Interactions between nuclei and the cytoskeleton are mediated by SUN-KASH nuclear-envelope bridges. *Ann. Rev. Cell Dev. Biol.* **26**, 421–444.

Tamura, K., Iwabuchi, K., Fukao, Y., Kondo, M., Okamoto, K., Ueda, H., Nishimura, M. and Hara-Nishimura, I. (2013) Myosin XI-I links the nuclear membrane to the cytoskeleton to control nuclear movement and shape in Arabidopsis. *Curr. Biol.* **23**, 1776–1781.

Tiang, C.L. (2010). The role of SYN1 in early *Arabidopsis* meiosis. Ph.D. thesis, University of Birmingham.

Tomita, K. and Cooper, J.P. (2006) The meiotic chromosomal bouquet: SUN collects flowers. *Cell*, **125**, 19–21.

Trelles-Sticken, E., Adelfalk, C., Loidl, J. and Scherthan, H. (2005) Meiotic telomere clustering requires actin for its formation and cohesin for its resolution. *J. Cell Biol.* **170**, 213–223.

Wilson, K.L. and Dawson, S.C. (2011) Functional evolution of nuclear structure. *J. Cell Biol.* **195**, 171–181.

Zhou, X. and Meier, I. (2013) How plants LINC the SUN to KASH. *Nucleus*, **4**, 206–215.

Zhou, X., Graumann, K., Evans, D.E. and Meier, I. (2012) Novel plant SUN–KASH bridges are involved in RanGAP anchoring and nuclear shape determination. *J. Cell Biol.* **196**, 203–211.

Zhou, X., Graumann, K., Wirthmueller, L., Jones, J.D.G. and Meier, I. (2014) Identification of unique SUN-interacting nuclear envelope proteins with diverse functions in plants. *J. Cell Biol.* **205**, 677–692.

Zickler, D. and Kleckner, N. (1998) The leptotene-zygotene transition of meiosis. *Ann. Rev. Genet.* **32**, 619–697.